J Mater Sci: Mater Electron (2023) 34:150

Structural and microwave dielectric properties of high-permittivity $Ca_{0.245}Li_{0.325}Nd_{0.395}Ti_{1-x}Sn_xO_3$ ceramics

Yeqing Guan[1], Jinxian Zhang[1], Fenglin Wang[1], Wei Li[1], Haijun Mao[1], Zhuofeng Liu[1], Weijun Zhang[1,*], and Xingyu Chen[1,*]

[1] College of Aerospace Science and Engineering, National University of Defense Technology, Changsha 410073, China

Received: 30 October 2022
Accepted: 21 December 2022
Published online: 17 January 2023

ABSTRACT

The $Ca_{0.245}Li_{0.325}Nd_{0.395}Ti_{1-x}Sn_xO_3$ (x = 0–0.12) ceramics were prepared by the traditional solid-state reaction method. The effects of Sn^{4+} substitution for Ti^{4+} on the phase composition, microstructure, and microwave dielectric properties of $Ca_{0.245}Li_{0.325}Nd_{0.395}Ti_{1-x}Sn_xO_3$ (CLNTSx) were investigated in this work. The X-ray diffraction results showed that the ceramics had a single orthorhombic perovskite structure when x = 0–0.09. However, a secondary phase SnO_2 was observed with $x > 0.09$. The SEM micrographs indicated that the proper Sn^{4+} substitution for Ti^{4+} promoted the grain growth and homogenization. The analysis results of Raman spectroscopy revealed the correlation between vibration modes and microwave dielectric properties of CLNTSx ceramics with different Sn^{4+} contents. The degree of cation order was related to the full width at half maximum (FWHM) of the Raman spectrum, and a lower FWHM value indicates higher cationic order and $Q \times f_0$ value. The excellent microwave dielectric properties with ε_r = 98, $Q \times f_0$ = 3320 GHz, and τ_f = 2.6 ppm/°C were obtained in the ceramics with x = 0.09 sintered at 1350 °C for 4 h.

1 Introduction

With the gradual commercialization of 5G communication technology and the continuous improvement of satellite communication systems, microwave dielectric ceramics as the basic materials for the preparation of the dielectric substrate, microwave antenna, resonator, filter, etc., play an important role in the field of wireless communication. Therefore, in order to meet the requirements of high frequency, high propagation speed, high reliability, and miniaturization, there is an urgent need to improve the properties of microwave dielectric ceramics, such as high permittivity (ε_r), high-quality factor ($Q \times f_0$), and near-zero resonant frequency temperature coefficient (τ_f) [1–5].

$CaTiO_3$ is an ABO_3 perovskite-typed ceramic and the basic forms of a wide range of dielectric ceramics, with a high permittivity of 170 and a medium $Q \times f_0$ value of 3600 GHz. The high permittivity of $CaTiO_3$ ceramic means that it is a potential candidate to meet the miniaturization requirements of microwave devices [6]. However, the large positive temperature coefficient of resonant frequency (τ_f = 800 ppm/°C)

Address correspondence to E-mail: zhwjun@nudt.edu.cn; chenxingyu@nudt.edu.cn

limits its development in practical application. In order to improve the microwave dielectric properties of $CaTiO_3$, especially to tune τ_f to near zero, many researchers had carried out a large number of experimental studies. Zhang and Xu [7, 8] used machine learning to predict the effect of ion substitution on oxygen ion conductivity and lattice constant of perovskite ceramics. Yoon et al. [9] had investigated the effect of A-site ions Ca^{2+}, Li^{+}, Sm^{3+} on the dielectric properties of $(1-x)Ca_{0.6}Sm_{0.67}TiO_3$–$xLi_{0.5}Sm_{0.5}TiO_3$ ceramics, and found that the composition with $x = 0.3$ exhibited the best microwave dielectric properties of $\varepsilon_r = 98$, $Q \times f_0 = 5100$ GHz, $\tau_f = 10$ ppm/°C. Kim et al. [10, 11] pointed out that the $Ca_{0.7}Nd_{0.2}TiO_3$ (CNT) ceramics could be compounded with $Li_{0.5}Nd_{0.5}TiO_3$ (LNT) ceramics to further improve the temperature stability. By adjusting the ratio between two raw ceramics, the dielectric materials with $\varepsilon_r = 130$, $Q \times f_0 = 2000$ GHz, $\tau_f > 15$ ppm/°C were produced at CNT:LNT = 1:1. Xiong et al. [12] studied the effect of $(Al_{0.5}Nb_{0.5})^{4+}$ on the microwave dielectric properties of $Ca_{0.61}Nd_{0.26}Ti_{1-x}(Al_{0.5}Nb_{0.5})_xO_3$ ceramics, founding that the introduction of $(Al_{0.5}Nb_{0.5})^{4+}$ improved the rigidity of oxygen octahedrons in the crystal structure. Moreover, the reduction reaction of Ti^{4+} at high temperature was suppressed, which helped to optimize its τ_f value and reduce the conductive loss. Xu et al. [13] revealed the relationship between the crystal structure and microwave properties of $Ca_{0.66}Nd_{0.34}Ti_{0.66}Al_{0.34}O_3$ ceramics by Raman scattering analysis. The ceramics sintered at 1500 °C had the best dielectric properties with $\varepsilon_r = 44.9$, $Q \times f_0 = 41{,}922$ GHz. Xiong et al. [14] investigated the effect of Mn^{4+}, Sn^{4+}, and Cr^{3+} ions on the structure of $Ca_{0.61}Nd_{0.26}TiO_3$ ceramics and found that different ionic substitutions led to oxygen octahedral distortion and changed the degree of cation order in the ceramic structure, thus improving the dielectric properties of the materials. Specifically, the quality factor of $Ca_{0.61}Nd_{0.26}Ti_{1-x}Sn_xO_3$ ceramics increased from 11,207 GHz at $x = 0$ to 14,369 GHz at $x = 0.01$. It can be seen from the above that the substitution of ions into the A/B-sites of $CaTiO_3$ can be a simple and effective way to improve the dielectric properties of microwave dielectric ceramics.

Therefore, attempts have been made to improve the dielectric properties of the $Ca_{0.245}Li_{0.325}Nd_{0.395}TiO_3$ ceramics by substituting Ti^{4+} with Sn^{4+}, so that it can maintain a high dielectric constant while having near-zero τ_f and low dielectric loss. These have been rare in reported dielectric ceramics with ε_r about 100. In this work, the effects of Sn substitution on the phase composition, microstructure, and microwave dielectric properties were investigated of $Ca_{0.245}Li_{0.325}Nd_{0.395}Ti_{1-x}Sn_xO_3$ ($x = 0$–0.12) ceramics, and the relationship between the lattice vibration modes and the microwave dielectric properties was also discussed.

2 Experimental procedure

The $Ca_{0.245}Li_{0.325}Nd_{0.395}Ti_{1-x}Sn_xO_3$ (CLNTSx) ($x = 0$–0.12) ceramics were prepared by the conventional solid-state reaction method. $CaCO_3$ (≥ 99.9%, Macklin Industrial Co.), Li_2CO_3 (≥ 99.0%, Aladdin Industrial Co.), Nd_2O_3 (≥ 99.99%, Aladdin Industrial Co.), TiO_2 (≥ 99.0%, Aladdin Industrial Co.), and SnO_2 (≥ 99.9%, Aladdin Industrial Co.) were used as raw materials. These materials were weighed according to the chemical formula $Ca_{0.245}Li_{0.325}Nd_{0.395}Ti_{1-x}Sn_xO_3$ ($x = 0$–0.12). Then, the powders were poured into a zirconia ball milling tank and milled for 4 h with anhydrous ethanol as the ball milling medium. After being dried and screened, the mixed raw material powders were placed in an alumina crucible calcined at 1100 °C for 3 h. After that, these calcined powders were milled again for 4 h. Subsequently, the powders were mixed with 5 wt% polyvinyl alcohol (PVA) to assist in pressing, then pressed into a cylindrical disk with a diameter of 13 mm and a thickness of 6–7 mm under 20 MPa. At last, these pellets were initially calcined at 450 °C for 1 h to burn out the organic binder, and then sintered at 1300–1375 °C for 4 h in air.

The bulk densities of samples were measured at room temperature by the Archimedes method. The crystalline phases were analyzed by an X-ray diffractometer (XRD, Rigaku, Smart Lab, Japan) with Cu Kα radiation generated under 45 kV and 200 mA. The microscopic morphology of the sample was observed by scanning electron microscope (SEM, MIRA4 LMH, TESCAN, Czech). The Raman spectrum of the sample was conducted on a Raman spectroscope (Raman, Renishaw InVia, UK) at room temperature with an Ar ion laser (532 nm) and collected in the range of 100–1000 cm^{-1}. The microwave dielectric properties of ceramics were measured by the parallel-plate dielectric resonator method using a

vector network analyzer (N5230C, Agilent, USA) in TE011 mode. The temperature coefficient of resonant frequency was calculated by the following formula:

$$\tau_f = \frac{f_{T2} - f_{T1}}{f_{T1}(T_2 - T_1)} \times 10^{-6}\ (\mathrm{ppm/^\circ C}),$$

where f_{T1}, f_{T2} are the resonant frequencies at T_1 (20 °C) and T_2 (80 °C), respectively.

3 Results and discussion

Figure 1a demonstrates the X-ray diffraction patterns of CLNTSx (x = 0–0.12) ceramics sintered at 1350 °C for 4 h. For compositions with x = 0–0.09, all reflection peaks were well indexed with orthorhombic perovskite structure (space group *Pbnm*(62), PDF#82-0228), which indicated that Sn^{4+} ions diffused into the lattice and formed a solid solution. However, a certain amount of diffraction peak belonging to SnO_2 (PDF#72-1147) was found when $x > 0.09$, which indicates that Sn^{4+} cannot be infinitely dissolved in the lattice. This result was consistent with results reported by Yan et al. [15] With the increasing Sn substitution, the (121) diffraction peaks at the position of 2θ = 33° are slightly shifted towards the low angle, as shown in Fig. 1b. According to Shannon's ionic radii table [16], the ionic radius of Sn^{4+} (0.69 Å, CN = 6) is larger than the ionic radius of Ti^{4+} (0.609 Å, CN = 6). Therefore, when Sn^{4+} diffused into the lattice, it was bound to increase the cell volume and the distance between crystal planes and made the diffraction peak shift to a low angle. To further analyze the effect of Sn^{4+} on the lattice constant and cell volume of the ceramic phase, the XRD data of the CLNTSx (x = 0–0.09) ceramics sintered at 1350 °C were refined by Rietveld refinement software (GSAS-EXPGUI). Figure 2 illustrates the Rietveld refinement diagram of the ceramic XRD (as an example), and Table 1 lists the relevant parameters obtained from the refinement. The reliability factor of the weighted pattern (R_{wp}) and reliability factor pattern (R_p) values are lower than 7%, and the goodness of fit indicator (χ^2) values are between 1.5 and 2.5. These results implied that a valid structural model and reliable Rietveld refinement results were obtained. As shown in Table 1, as the x value increased, the lattice parameters (a, b, c) of CLNTSx ceramics continued to increase, resulting in an increase in cell volume (V_{cell}) from 224.3669 to 225.2898 $Å^3$. These indicate that the Sn was diffused into the crystal lattices, and a solid solution is completely formed when $x \leq 0.09$.

Figure 3 exhibits the microstructures of CLNTSx ceramics with various x values sintered at 1350 °C for 4 h. It was observed that all the samples

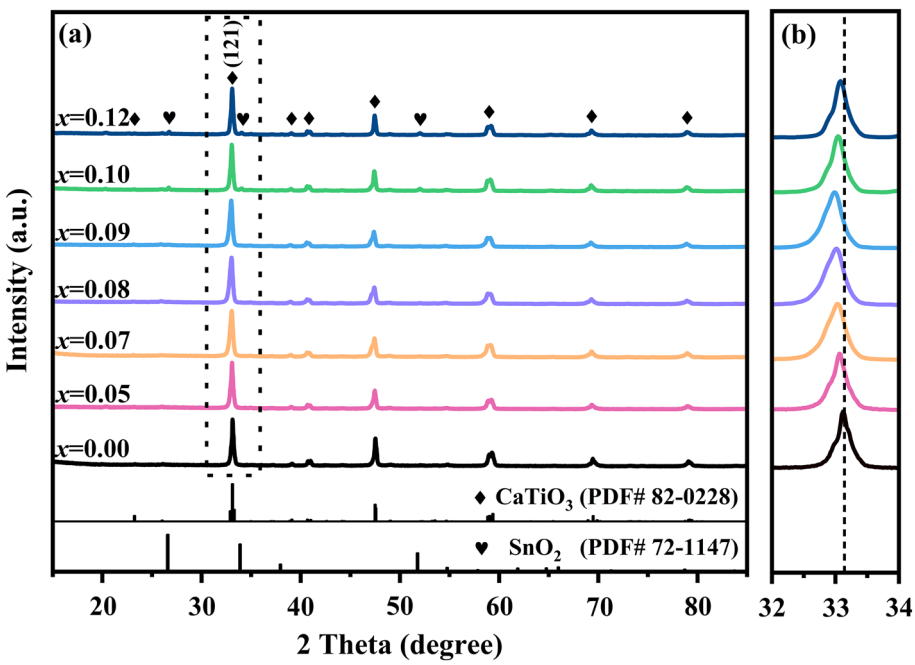

Fig. 1 XRD patterns of $Ca_{0.245}Li_{0.325}Nd_{0.395}Ti_{1-x}Sn_xO_3$ (x = 0–0.12) ceramics sintered at 1350 °C for 4 h

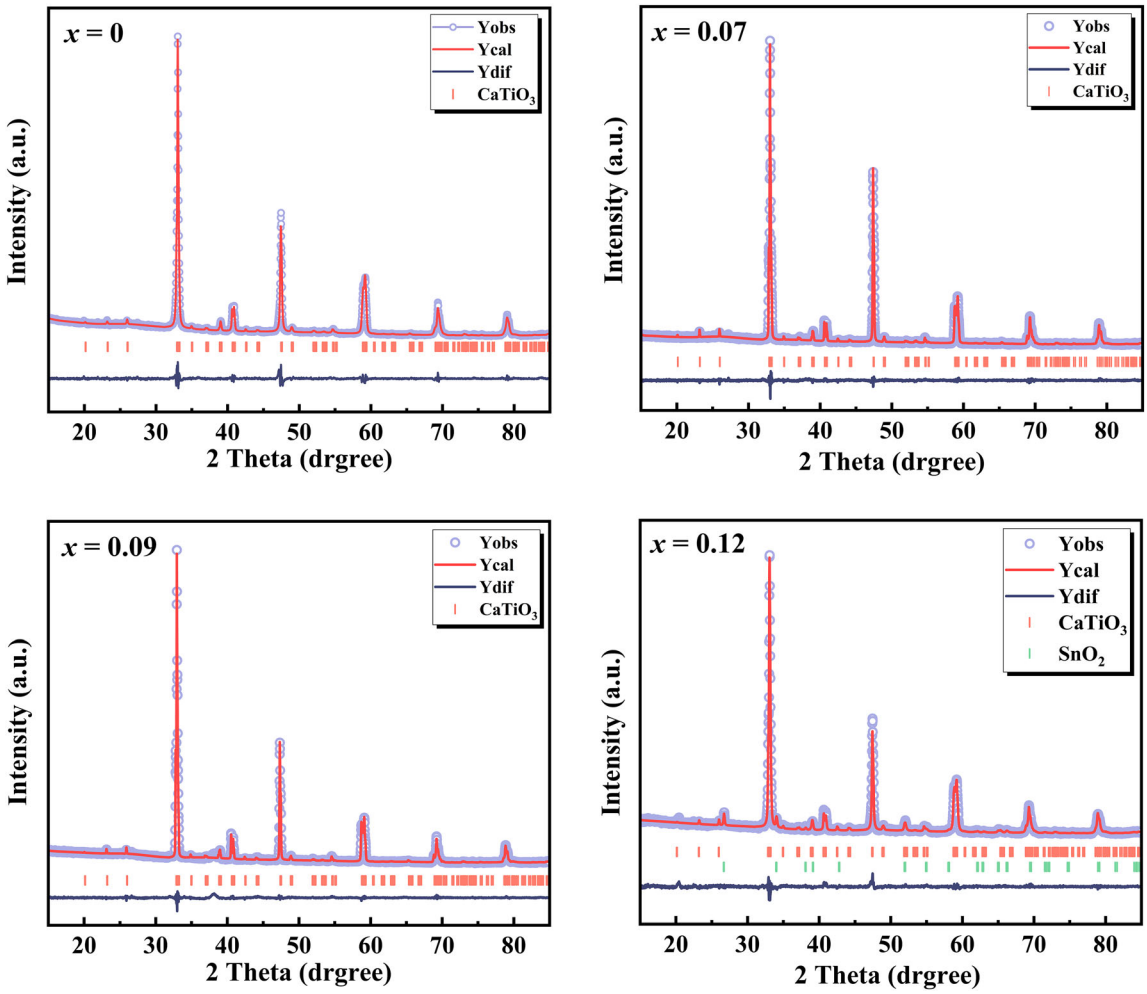

Fig. 2 Rietveld refinement patterns for CLNTSx (x = 0, 0.07, 0.9, 0.12)

Table 1 Lattice parameters and reliability factors of $Ca_{0.245}Li_{0.325}Nd_{0.395}Ti_{1-x}Sn_xO_3$ ($0 \le x \le 0.09$) ceramics

x	a (Å)	b (Å)	c (Å)	V_{cell} (Å^3)	R_{wp} (%)	R_p (%)	χ^2
0	5.3897 (1)	5.4395 (4)	7.6529 (9)	224.3667 (0)	4.97	3.40	2.06
0.05	5.3909 (3)	5.4429 (3)	7.6649 (1)	224.9084 (0)	6.84	4.76	2.41
0.07	5.3918 (5)	5.4450 (2)	7.6648 (3)	225.0290 (3)	4.92	3.75	1.62
0.08	5.3929 (4)	5.4452 (7)	7.6653 (5)	225.1010 (3)	4.60	3.55	1.53
0.09	5.3950 (5)	5.4463 (6)	7.6672 (5)	225.2904 (4)	4.75	3.20	1.84

have a clear microstructure and obvious grain boundaries. Moreover, with the increase of the x value, the grain size becomes uniform and the porosity at the grain boundaries decreases gradually, which indicated that a certain of Sn^{4+} was beneficial to the formation of uniform and dense microstructure. The energy dispersive X-ray spectroscopy (EDS) was utilized to further reveal the microscopic information of CLNTSx (x = 0, 0.1), as shown in Fig. 3h, i. According to the EDS spectra of grains A and B, the ratios of Ca: Nd: (Ti + Sn) were close to 1:1.6:4.1. This also proved that the Sn^{4+} ion has successfully replaced the Ti^{4+} ion at the B-site. The bulk density and relative density are shown in Fig. 4. The bulk density had an obvious upward trend when $0 \le x \le 0.09$, mainly because the relative atomic mass of Sn was slightly larger than that of Ti. Therefore, the density of CLNTSx ceramics substituted with a small

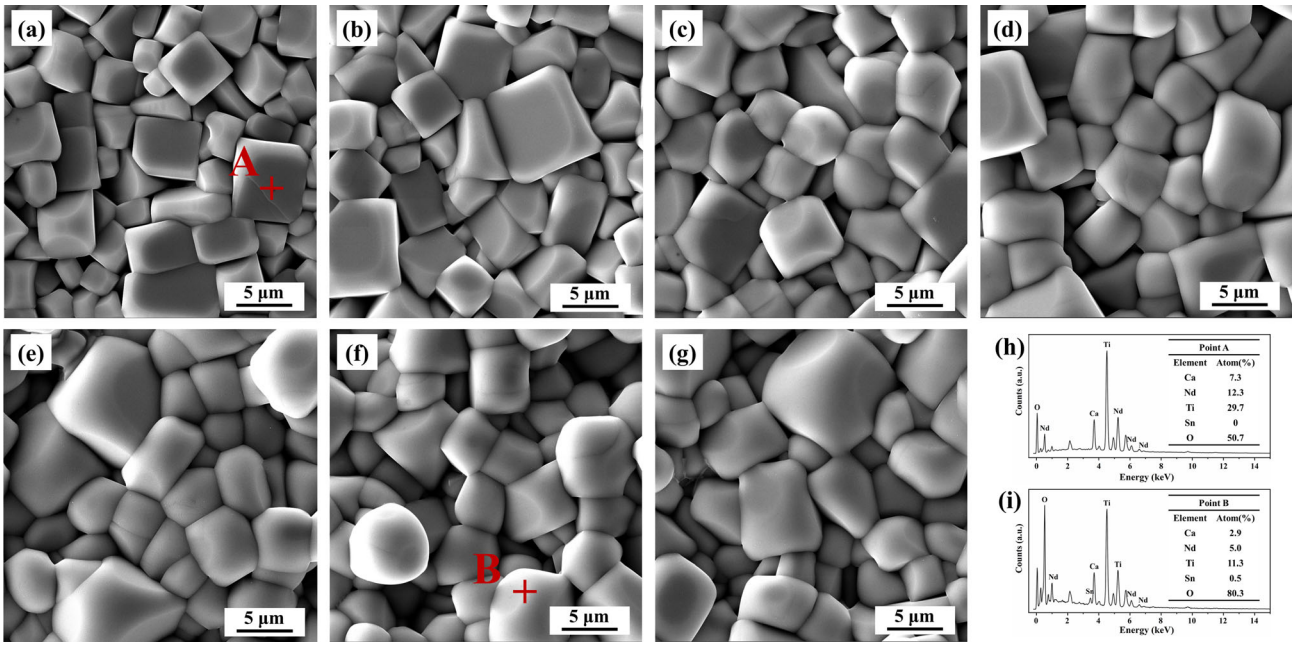

Fig. 3 The SEM images of CLNTSx (x = 0–0.12) ceramics sintered at 1350 °C for 4 h with different x content: **a** x = 0, **b** x = 0.05, **c** x = 0.07, **d** x = 0.08, **e** x = 0.09, **f** x = 0.1, **g** x = 0.12; and the EDS results of surface scanning: **h**: grain A, and **i** grain B

amount of Sn changes considerably compared with that of unsubstituted ceramics. But when $x > 0.09$, the density of CLNTSx ceramics decreased slightly due to the increase in surface porosity. The inset in Fig. 4 shows the relative densities of all samples sintered at 1350 °C. The relative densities of all samples are higher than 96%, which is consistent with the dense micro-structure of the ceramics shown in the SEM images.

In order to explore the relationship between the crystal structure and microwave dielectric properties of the ceramics, the mechanism of the substitution of Sn^{4+} for Ti^{4+} on the crystal structure of CLNTSx ceramics was further analyzed by Raman spectroscopy. According to the crystal space group theory, there are 24 different Raman-activity modes ($\Gamma = 7A_g + 5B_{1g} + 7B_{2g} + 5B_{3g}$) in ceramics with orthorhombic perovskite structure [17, 18]. However, because some bands overlapped with other stronger bands, only parts of these Raman modes can be observed in the practical spectra. The room temperature Raman spectra of CLNTSx (x = 0–0.12) in the range of 100–900 cm^{-1} are shown in Fig. 5, and the spectrum was similar to those results of many reported $CaTiO_3$-base materials in previous investigations [14, 19, 20]. There were seven different bands in the spectrum at 153, 238, 362, 467, 539, 675, and 748 cm^{-1}. Compared with previous studies, the band at 153 cm^{-1} was

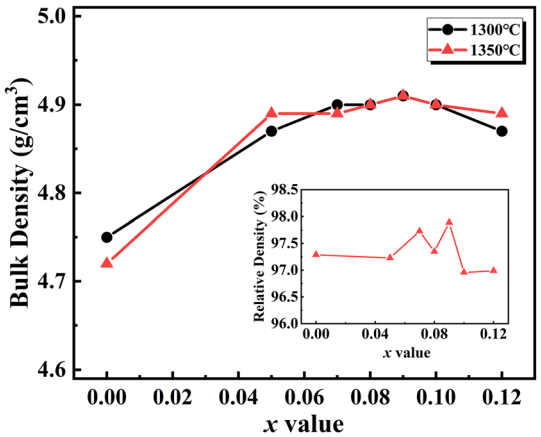

Fig. 4 The bulk density of CLNTSx (x = 0–0.12) ceramics sintered at different temperatures with different x content, and the relative density of the samples sintered at 1350 °C (illustration)

associated with the motion of A-site ions, and the bands in the region of 238–362 cm^{-1} were assigned to the rotational vibration of oxygen octahedrons. The bands at 467 cm^{-1} and 539 cm^{-1} were caused by the vibration of ions in the oxygen octahedron. The bands at 675 cm^{-1} and 748 cm^{-1} could be attributed to the stretching vibration of the Ti–O bond, which generally appears in the complex perovskite [20, 21]. In the range of x from 0 to 0.09, the band at 362 cm^{-1} became wider and weaker with increasing x values, which indicated that the vibration modes related to

the rotation of oxygen octahedron in ceramics weaken and the rigidity of oxygen octahedron network structure increased. The band at 539 cm^{-1} gradually became narrower and weaker due to the increase of oxygen octahedron distortion, resulting in the limitation of ion displacement vibration and the weakening of peak intensity. According to previous reports, the peak width was related to the order of ion occupation, and the narrower peak width meant a higher cation order [22, 23]. When $x > 0.09$, the bands at 362 cm^{-1} and 539 cm^{-1} became sharp again, which may be related to the appearance of the second phase of SnO_2. It is generally believed that the full width at half maximum (FWHM) of the band is closely associated with microwave dielectric properties. The FWHM of the band at 539 cm^{-1} decreased from 66.32 cm^{-1} at $x = 0$ to 59.19 cm^{-1} at $x = 0.09$, and increased to 62.09 cm^{-1} at $x = 0.12$. This suggested that CLNTSx ceramics had a higher degree of cation order at $x = 0.09$. To a certain extent, the increase of the order degree of cations is beneficial to reduce the dielectric loss of ceramics.

Figure 6 shows the dielectric constants of CLNTSx (x = 0–0.12) ceramics sintered at different temperatures as a function of the x value. The dielectric constants of the ceramics decreased gradually with the increase of the x value. This trend in the change of dielectric constant with substituted ions has been reported similarly in previous investigations [24, 25]. Generally, the dielectric constant is usually affected by various factors such the relative density, phase composition, pore, and ionic polarizability [26–28]. In this work, the relative densities of the samples were all above 97% and tended to be stable. Therefore, the effect of density on dielectric properties can be ignored, and the variation of ε_r of CLNTSx (x = 0–0.09) ceramics was mainly dependent on ionic polarizability and phase composition. According to the Clausius–Mosotti equation (Eq. 1), the dielectric constant was closely related to the ionic polarizability and molecular molar volume:

$$\varepsilon_r = \frac{3V_m + 8\pi\alpha_D^T}{3V_m - 4\pi\alpha_D^T}. \quad (1)$$

If $b = 4\pi/3$, the equation can be simplified as follows:

$$\varepsilon_r = \frac{1 + 2b\alpha_D^T/V_m}{1 - b\alpha_D^T/V_m}, \quad (2)$$

where ε_r, V_m, α_D^T are the theoretical dielectric constant, the molecular molar volume per unit cell, and the ionic polarizability, respectively. Where α_D^T can be obtained via the following Shannon's summation rule:

$$\begin{aligned}\alpha_D^T = {} & 0.245\alpha(Ca^{2+}) + 0.395\alpha(Nd^{3+}) \\ & + 0.325\alpha(Li^{+}) + x\alpha(Sn^{4+}) \\ & + (1-x)\alpha(Ti^{4+}) + 3\alpha(O^{2-}).\end{aligned} \quad (3)$$

According to the ionic polarizability data given by Shannon [25]. This causes the α_{theo} (Å^3) to decrease linearly with the increase of the x value (as shown in the illustration in Fig. 6). And the ionic radius of Sn^{4+} (0.69 Å, CN = 6) is larger than the ionic radius of Ti^{4+} (0.609 Å, CN = 6). This will inevitably lead to an

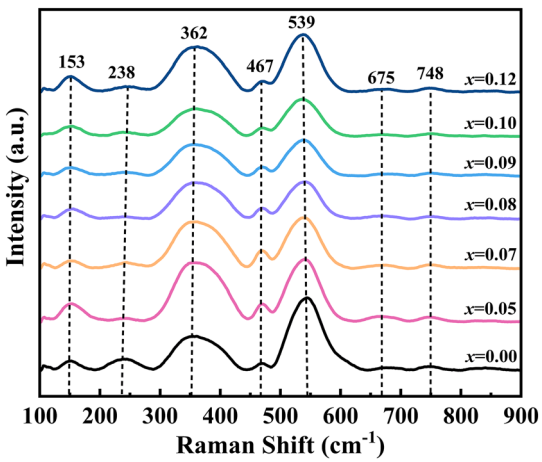

Fig. 5 Raman spectra of CLNTSx (x = 0–0.12) ceramics sintered at 1350 °C

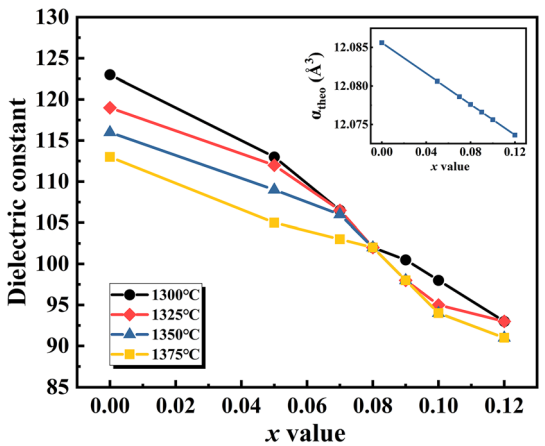

Fig. 6 The ε_r of the CLNTSx (x = 0–0.12) ceramics sintered at different temperatures; dielectric polarizabilities α_{theo} (Å^3) for CLNTSx ceramics (illustration)

increase in cell volume (V_m), as shown in Table 1. Therefore, as the value of x increased, the α_D^T of the samples decreased and the V_m increased, as can be seen from Eq. 2, which eventually lead to a decrease in the dielectric constant. On the other hand, as the analysis of Raman spectra above, the oxygen octahedral aberration rate increased due to the substitution of Sn^{4+} for Ti^{4+}, then the coordination environment of the B-site changed. The polarizability of the ions in the crystal may be affected by the coordination environment [29], which leads to a decrease in the effective ion polarizability. This may also be the reason for the decrease in the dielectric constant.

Figure 7 exhibits the quality factors of CLNTSx (x = 0–0.12) ceramics sintered at different temperatures. It can be noted that an appropriate amount of Sn^{4+} substitution for Ti^{4+} was beneficial to improve the $Q \times f_0$ value of the ceramics. After the ceramics were sintered at 1350 °C, the quality factors increased from 2210 GHz for the unsubstituted sample (x = 0) to 3320 GHz at the composition x = 0.09, and then gradually decreased with further increase in x values. In the microwave frequency band, the dielectric loss of dielectric materials can be divided into intrinsic factors and extrinsic factors. The intrinsic factors were mainly caused by the anharmonic vibration in the crystal structure and even existed in an ideal crystal, which cannot be completely avoided. The extrinsic factors were mainly related to the lattice defects of the material, such as porosity, impurity, grain size, and second phase [30, 31]. From the microstructure in Fig. 3, with the increase of x value,

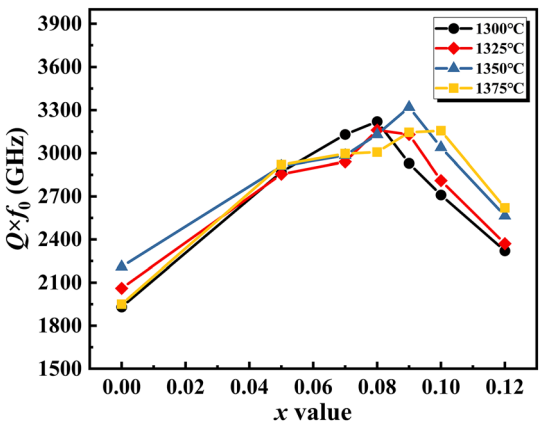

Fig. 7 The $Q \times f_0$ value of the CLNTSx (x = 0–0.12) ceramics sintered at different temperatures

the porosity of ceramics decreased and the surface morphology tended to be densified, which indicated that an appropriate amount of Sn^{4+} substitution for Ti^{4+} helps to improve the quality factor of the ceramics. In addition, the trend of the $Q \times f_0$ value was opposite to that of the FWHM of Raman, which indicated that the quality factor of the ceramics was closely related to the FWHM of the Raman peaks. As previously analyzed, the improved quality factor was related to the improvement of the cationic order of the CLNTSx ceramics. In this work, the sintering temperatures of these ceramics were higher than 1300 °C. At high temperatures, a small amount of oxygen breaks away from the bondage of the lattice to produce oxygen vacancies and weakly bound electrons, which may lead to a partial reduction of Ti^{4+} to Ti^{3+} ions and reduce the quality factor of ceramics. With the substitution of Sn^{4+} for Ti^{4+}, the quality factor of the CLNTSx ceramics was optimized due to the following reaction that helped to suppress the reduction of Ti^{4+} [32, 33].

$$O_O^{\times} \rightarrow V_{\ddot{O}} + 2e' + \frac{1}{2}O_2,$$
$$Ti^{4+} + e' \rightarrow Ti^{3+},$$
$$Sn^{4+} + Ti^{3+} \rightleftharpoons Sn^{3+} + Ti^{4+}.$$

However, upon a further increase in Sn^{4+} content ($x > 0.09$), the excessive substitution leads to a decrease in the density and an increase in the porosity of the ceramic, accompanied by the appearance of the second phase of SnO_2. These phenomena may be the reasons for the decrease in the $Q \times f_0$ value of the CLNTSx ceramics.

Figure 8 shows the variation of the temperature coefficient of resonant frequency (τ_f) with x of CLNTSx (x = 0–0.12) ceramics after sintering at the optimum temperature for 4 h. With increasing x value, the τ_f decreased from 21.1 to 2.6 ppm/°C. Through the study of the dielectric properties of a large number of binary/multicomponent compounds, the empirical formulas of τ_f value, the temperature coefficients of dielectric constants (τ_ε), and the thermal expansion coefficients (α_L) were summarized, as follows:

$$\tau_f = -\left(\alpha_L + \frac{\tau_\varepsilon}{2}\right), \quad (4)$$

where the α_L does not deviate from 8 to 10 ppm/°C for perovskite structure [4], which means that the τ_f value of ceramics is mainly affected by τ_ε. Furthermore, researchers had revealed that the dielectric properties of perovskite ceramics, especially τ_f, are mainly affected by oxygen octahedrons. Reaney [4] proposed a hypothesis that the structural tolerance factor (t) affects the τ_f of microwave dielectric ceramics with perovskite structure by controlling the phase transition temperature. Lower t values favor distorted structures that have undergone phase transition involving the rotation of oxygen octahedrons at lower temperatures. Moreover, Colla et al. [34] proved that the variation of τ_ε of complex perovskites was directly related to the tilt of the oxygen octahedron, and the tolerance factor can affect the tilt of the oxygen octahedron. Therefore, the τ_f value of CLNTSx ceramics can be considered to be mainly affected by the tolerance factor (t). The t is defined as follows:

$$t = \frac{R_A + R_O}{\sqrt{2}(R_B + R_O)}, \quad (5)$$

where R_A, R_B, and R_O were the average ionic radii of A-site ions, B-site ions, and oxygen ions, respectively. The trend of tolerance factors was shown in Fig. 8. It can be seen that the τ_f value of CLNTSx ceramics was related to the tolerance factor when $x \leq 0.09$, but upon a further increase in Sn content ($x > 0.09$), the increase of τ_f may be related to the appearance of second phase SnO_2.

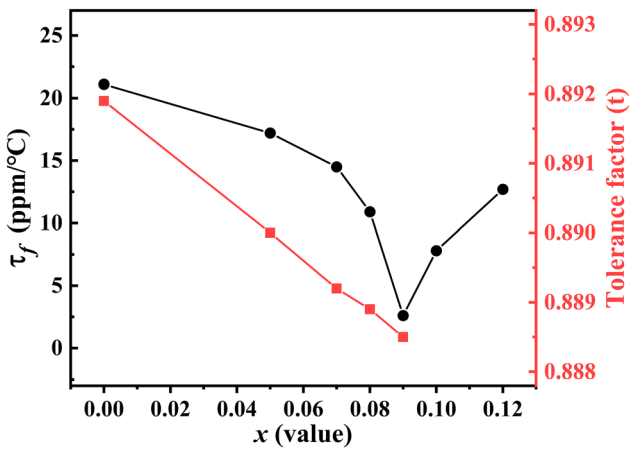

Fig. 8 The τ_f value and tolerance factor of the CLNTSx (x = 0–0.12) ceramics sintered at different temperatures

In this contribution, we have demonstrated that the use of a small amount of Sn ($x \leq 0.09$) instead of Ti can effectively tune the τ_f of $Ca_{0.245}Li_{0.325}Nd_{0.395}Ti_{1-x}Sn_xO_3$ ceramics to near zero without significantly deteriorating the dielectric constant. Although the $Q \times f_0$ value of 3320 GHz for Sn-substituted sample is not as high as many microwave dielectric ceramics, it has been quite rare in reported dielectric ceramics with ε_r of ~ 100 and τ_f close to zero. One of the ways to improve the quality factor of perovskite ceramics is to reduce the oxygen vacancies (V_o) during high-temperature sintering. Our recent research found that sintering or annealing in oxygen-rich atmospheres can effectively reduce the V_o concentration in ceramics due to the oxygen compensation effect. This method can double the quality factor of the material without affecting the dielectric constant. Therefore, the mechanism of how atmosphere sintering improves the microwave dielectric properties of perovskite ceramics will be the subject of further study.

4 Conclusion

The effect of Sn^{4+} substitution on the phase composition, microstructure, and microwave dielectric properties of $Ca_{0.245}Li_{0.325}Nd_{0.395}Ti_{1-x}Sn_xO_3$ (x = 0–0.12) ceramics was investigated. With a small amount of Sn substitution ($x \leq 0.09$), the ceramics exhibited a single phase with an orthorhombic perovskite structure, and too much substitution (x = 0.1–0.12) resulted in the appearance of a secondary phase SnO_2. The degree of oxygen octahedral distortion and the order degree of cations in CLNTSx varied with Sn^{4+} contents. For compositions where $x \leq 0.09$, the ε_r value gradually decreased with increasing Sn substitution, which was related to the smaller ionic polarizability of Sn^{4+} compared to Ti^{4+}. The $Q \times f_0$ value greatly depended on the order degree of cations and the secondary phase SnO_2. Moreover, the inhibition of Ti^{4+} reduction by Sn^{4+} at high temperatures will also affect the $Q \times f_0$ value of the ceramics. The τ_f was greatly affected by the variation of tolerance factor and the appearance of secondary phase. At the composition x = 0.09, the CLNTSx ceramics achieved the best microwave dielectric properties at the sintering temperature of 1350 °C with a permittivity of 98, a $Q \times f_0$ value of 3320 GHz, and a near-zero τ_f of 2.6 ppm/°C.

Author contributions

YG performed the experiments, data analysis and wrote the manuscript. JZ made an important contribution to the experimental work. XC and FW contributed to the data analysis and manuscript preparation significantly. WL, HM and ZL helped to perform the data analysis with constructive discussions. WZ contributed to the conception of the study.

Funding

This work is supported by the Natural Science Foundation of Hunan Province of China (Grant No. 2022JJ30661), the Natural Science Foundation of Hunan Province of China (Grant No. 2022JJ40549), the National Natural Science Foundation of China (Grant No. 11705281) and the Research Project of National University of Defense Technology (ZK22-54).

Data availability

The authors declare that all data generated during the study appear in the submitted article.

Declarations

Conflict of interest The authors have no conflicts of interest to declare that are relevant to the content of this article.

References

1. H. Yang, S. Zhang et al., The latest process and challenges of microwave dielectric ceramics based on pseudo phase diagrams. J. Adv. Ceram. **10**, 885–932 (2021)
2. M.T. Sebastian, R. Ubic et al., Low-loss dielectric ceramic materials and their properties. Int. Mater. Rev. **60**, 392–412 (2015)
3. M.T. Sebastian, H. Jantunen, Low loss dielectric materials for LTCC applications: a review. Int. Mater. Rev. **53**, 57–90 (2013)
4. I.M. Reaney, Microwave dielectric ceramics for resonators and filters in mobile phone networks. J. Am. Ceram. Soc. **89**(7), 2063–2072 (2006)
5. Z. Lou, Q. Wang et al., Regulating lignin content to obtain excellent bamboo-derived electromagnetic wave absorber with thermal stability. Chem. Eng. J. **430**, 133178 (2022)
6. H. Kagata, J. Kato, Dielectric properties of Ca-based complex perovskite at microwave frequencies. JJAP **33**, 5463–5465 (1994)
7. Y. Zhang, X. Xu, Modeling oxygen ionic conductivities of ABO_3 perovskites through machine learning. Chem. Phys. **558**, 111511 (2022)
8. Y. Zhang, X. Xu, Modeling of lattice parameters of cubic perovskite oxides and halides. Heliyon **7**, e07601 (2021)
9. K.H. Yoon, Y.H. Chang et al., Dielectric properties of $Ca_{0.6}$-$Sm_{0.267}TiO_3$–$Li_{0.5}Ln_{0.5}TiO_3$ ceramics. JJAP **35**, 5145–5149 (1996)
10. E.S. Kim, B.S. Chun et al., Microwave dielectric properties of $(1–x)(Ca_{0.7}Nd_{0.2})TiO_3$–$x(Li_{0.5}Nd_{0.5})TiO_3$ ceramics. Mater. Sci. Eng. B **99**, 247–251 (2003)
11. K. Ezaki, Y. Baba et al., Microwave dielectric properties of $CaO–Li_2O–Nd_2O_3–TiO_2$ ceramics. JJAP **32**, 4319–4322 (1993)
12. Z. Xiong, X. Zhang et al., Characterization of structural and electrical properties of $Ca_{0.61}Nd_{0.26}TiO_3$ ceramic tailored by complex ions $(Al_{0.5}Nb_{0.5})^{4+}$. J. Alloys Compd. **899**, 163434–163245 (2022)
13. Y. Xu, R. Fu et al., Sintering behavior, microwave dielectric properties of $Ca_{0.66}Ti_{0.66}Nd_{0.34}Al_{0.34}O_3$ ceramics revealed by microstructure and Raman scattering. J. Alloys Compd. **785**, 335–342 (2019)
14. Z. Xiong, B. Tang et al., Different additives doped Ca–Nd–Ti microwave dielectric ceramics with distorted oxygen octahedrons and high Q × f value. ACS Omega **3**, 11033–11040 (2018)
15. Y. Yan, Z. Li et al., Preparation and microwave dielectric properties of $Ca_{0.6}La_{0.8/3}$ $(Sn_xTi_{1-x})O_3$ ceramics. Ceram. Int. **43**, 8534–8537 (2017)
16. R.D. Shannon, Revised effective ionic radii and systematic studies of interatomic distances in halides and chalcogenides. Acta Crystallogr. A **32**, 751–767 (1976)
17. R. Lowndes, M. Deluca et al., Probing structural changes in $Ca_{(1-x)}Nd_{2x/3}TiO_3$ ceramics by Raman spectroscopy. J. Appl. Phys. **113**(4), 044115 (2013)
18. H. Zheng, I.M. Reaney et al., Raman spectroscopy of $CaTiO_3$-based perovskite solid solutions. J. Mater. Res. **19**, 488–495 (2003)
19. M.S. Fu, X.Q. Liu et al., Raman spectra analysis for $Ca(B_{1/3'}B_{2/3''})O_3$-based complex perovskite ceramics. J. Appl. Phys. **104**(10), 104108 (2008)
20. H. Zheng, C. de Györgyfalva et al., Raman spectroscopy of B-site order–disorder in $CaTiO_3$-based microwave ceramics. J. Eur. Ceram. Soc. **23**, 2653–2659 (2003)

21. S. Liu, B. Tang et al., Microwave dielectric characteristics of high permittivity $Ca_{0.35}Li_{0.25}Nd_{0.35}Ti_{1-x}(Zn_{1/3}Ta_{2/3})_xO_3$ ceramics (x = 0.00–0.12). Ceram. Int. **45**, 8600–8606 (2019)
22. Z. Xiong, C. Yang et al., Structure–property relationships of perovskite-structured $Ca_{0.61}Nd_{0.26}Ti_{1-x}(Cr_{0.5}Nb_{0.5})_xO_3$ ceramics. Ceram. Int. **44**, 7384–7392 (2018)
23. Z. Xiong, B. Tang et al., Effects of $(Cr_{0.5}Ta_{0.5})^{4+}$ on structure and microwave dielectric properties of $Ca_{0.61}Nd_{0.26}TiO_3$ ceramics. Ceram. Int. **44**, 7771–7779 (2018)
24. Z. Fang, B. Tang et al., Microstructures and microwave dielectric properties of $Na_{0.5}Nd_{0.2}Sm_{0.3}Ti_{1-x}Sn_xO_3$ ceramics (x = 0.00 to 0.50). J. Electron. Mater. **44**, 4236–4242 (2015)
25. L. Veselinović, M. Mitrić et al., The effect of Sn for Ti substitution on the average and local crystal structure of $BaTi_{1-x}Sn_xO_3$ ($0 \leq x \leq 0.20$). J. Appl. Crystallogr. **47**, 999–1007 (2014)
26. B. Ullah, A. Sayyadi-Shahraki et al., Dielectric abnormality and high-permittivity microwave dielectric properties of SrO–TiO_2–CeO_2 solid solution. Ceram. Int. **45**, 3634–3642 (2019)
27. F. Liu, J.J. Qu et al., Phase structures, microstructures, and dielectric characteristics of high εr $(1–x–y)Bi_{0.5}Na_{0.5}TiO_3$–$xLi_{0.5}Sm_{0.5}TiO_3$–$yNa_{0.5}La_{0.5}TiO_3$ microwave ceramic systems. Ceram. Int. **45**, 7839–7849 (2019)
28. R.D. Shannon, Dielectric polarizabilities of ions in oxides and fluorides. J. Appl. Phys. **73**, 348–366 (1992)
29. M.W. Lufaso, Crystal structures, modeling, and dielectric property relationships of 2:1 ordered $Ba_3MM'_2O_9$ (M = Mg, Ni, Zn; M′ = Nb, Ta) perovskites. Chem. Mater. **16**, 2148–2156 (2004)
30. X.Q. Song, C.Z. Yin et al., Structural evolution and microwave dielectric properties of $CaTiO_3$–$La(Mg_{2/3}Nb_{1/3})O_3$ ceramics. J. Am. Ceram. Soc. **105**(12), 7415–7425 (2022)
31. L. Shi, R. Peng et al., Effects of magnesium–tungsten co-substitution on crystal structure and microwave dielectric properties of $CaTi_{1-x}(Mg_{1/2}W_{1/2})xO_3$ ceramics. Ceram. Int. **47**, 3354–3360 (2021)
32. A. Ali, S. Uddin et al., Structural, optical and microwave dielectric properties of $Ba(Ti_{1-x}Sn_x)4O_9$, $0 \leq x \leq 0.7$ ceramics. Sci. Rep. **11**, 17889 (2021)
33. B. Huang, Z. Yan et al., "Dark hole" cure in $Ba_{4.2}Nd_{9.2}$-$Ti_{18}O_{54}$ microwave dielectric ceramics. Ceram. Int. **42**, 10758–10763 (2016)
34. E.L. Colla, I.M. Reaney et al., Effect of structural changes in complex perovskites on the temperature coefficient of the relative permittivity. J. Appl. Phys. **74**, 3414–3425 (1993)